JACS
JOURNAL OF THE AMERICAN CHEMICAL SOCIETY
pubs.acs.org/JACS
Article

Development of FBXO22 Degraders and the Recruitment Ligand 2-Pyridinecarboxyaldehyde (2-PCA)

Tian Qiu,[▽] Zhe Zhuang,[▽] Woong Sub Byun,[▽] Zuzanna Kozicka,[▽] Kheewoong Baek, Jianing Zhong, Abby M. Thornhill, Julia K. Ryan, Katherine A. Donovan, Eric S. Fischer, Benjamin L. Ebert,* and Nathanael S. Gray*

Cite This: https://doi.org/10.1021/jacs.5c14141
Read Online

ACCESS | Metrics & More | Article Recommendations | Supporting Information

ABSTRACT: Targeted protein degradation (TPD) is a promising therapeutic strategy that requires the discovery of small molecules that induce the proximity between E3 ubiquitin ligases and proteins of interest. FBXO22 is an E3 ligase that is overexpressed in many cancers and implicated in tumorigenesis. While FBXO22 was previously identified as capable of recognizing ligands bearing a primary amine degron, further investigation and development of recruitment ligands are required to enable its broader utility for TPD. Here, we describe the discovery of chemical probes that can either selectively degrade FBXO22 or recruit this ligase for TPD applications. First, we described AHPC(Me)-C6-NH_2 as a potent and selective FBXO22 degrader (DC_{50} = 77 nM, D_{max} = 99%) that is suitable for interrogating the effects of FBXO22 loss of function. Further, we discovered that the simple hexane-1,6-diamine acts as a minimal FBXO22 self-degrader, whereas shorter C4 (putrescine) to C5 (cadaverine) analogs, found in mammalian cells, do not induce degradation. Finally, we found that 2-pyridinecarboxaldehyde (2-PCA) functions as a novel electrophilic degron capable of forming a reversible thioacetal with cysteine 326 for recruiting FBXO22. Conjugating 2-PCA to various ligands successfully induced the FBXO22-dependent degradation of BRD4 and CDK12. Collectively, these chemical probes will facilitate the study of FBXO22 biology and broaden its applicability in the TPD.

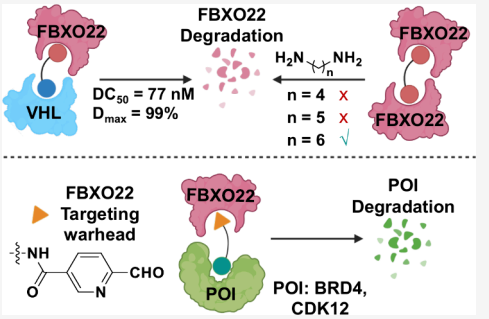

INTRODUCTION

Targeted protein degradation (TPD) has emerged as a compelling alternative to conventional small-molecule inhibition by harnessing the cell's natural ubiquitin−proteasome system (UPS) to eliminate proteins of interest (POIs).[1−3] Unlike traditional inhibitors that merely block protein activity, TPD removes the entire protein, thereby, abolishing its functions and interactions. TPD primarily employs two types of small molecules: (1) heterobifunctional proteolysis-targeting chimeras (PROTACs), which connect a POI-binding ligand to an E3 ligase recruiter via a suitable linker;[4,5] and (2) molecular glue degraders (MGDs), which use a monovalent ligand to stabilize interactions between a POI and an E3 ligase.[6,7] Both strategies promote ternary complex formation, polyubiquitination, and subsequent proteasome-mediated degradation. Despite the growing repertoire of degradable proteins, most TPD approaches still rely on recruiting either cereblon (CRBN)[8] or von Hippel−Lindau (VHL)[9] due to the availability of well-described ligands for these ligases. This overreliance presents several challenges, including suboptimal degradation of certain proteins due to incompatible surface topologies, limited expression of CRBN or VHL in some cell types, and the resistance induced by reduced expression of the E3.[10−12] These limitations underscore the need to identify and validate additional ligandable E3 ligases to expand the therapeutic potential of TPD.

The UPS is a central regulator of protein homeostasis and a validated therapeutic target, as demonstrated by the clinical success of proteasome inhibitors in oncology. However, these agents often exert broad effects leading to proteotoxic stress, highlighting the need for more selective approaches.[13] Targeting E3 ubiquitin ligases, the components that confer substrate specificity within the UPS, offers a more precise strategy. E3 ligases play critical roles in diverse cellular processes and have been implicated in cancer, neurodegeneration, and inflammatory diseases.[14−16] Yet, most E3 ligases remain pharmacologically inaccessible due to the lack of well-defined ligandable pockets. To date, the few available E3 ligase inhibitors—including those directed at MDM2,[17] IAPs,[18,19] VHL,[20,21] and KEAP1[22]—primarily function by disrupting protein−protein interactions (PPIs) with substrates. Despite progress, there

Received: August 14, 2025
Revised: November 7, 2025
Accepted: November 10, 2025

remains a stark gap between the number of known human E3 ligases and the small fraction currently targeted by drug-like molecules. Recently, small-molecule degraders of E3 ligases have emerged as a promising alternative modality.[23] Still, their broader application is limited by the scarcity of validated ligands for most E3 ligases. These challenges underline the need to develop both ligands and degraders targeting therapeutically relevant E3 ligases.

FBXO22 (F-box only protein 22) exemplifies this opportunity and has recently emerged as a promising E3 ligase for TPD applications.[24−28] As a member of the F-box protein family, FBXO22 functions as the substrate receptor for an SCF (SKP1−CUL1−F-box protein) E3 ubiquitin ligase complex. FBXO22 has been implicated in the development and progression of multiple cancers, including liver,[29] colorectal,[30] breast cancers[31] and leukemia.[32] Analysis of The Cancer Genome Atlas (TCGA) data revealed that FBXO22 mRNA levels are significantly upregulated in a range of human tumor tissues compared to corresponding normal tissues.[33] Functionally, FBXO22 regulates key processes such as cell cycle progression, DNA damage response, and chromatin remodeling by targeting tumor suppressors, transcriptional regulators including the cyclin-dependent kinase inhibitor p21,[29] and the histone demethylase KDM4A.[34,35] A particularly well-characterized substrate is the transcription factor BACH1 (BTB and CNC homology 1), which plays a key role in orchestrating oxidative stress adaptation.[32,36] Recent structural studies have revealed how FBXO22 recognizes a heme-regulated degron within the C-terminal region of BACH1, establishing a direct link between cellular heme levels and BACH1 stability.[37,38] Chemical modulation of FBXO22 activity could serve as a valuable tool to further dissect its biological functions. In addition, given the elevated level of expression in cancer cells, FBXO22 represents an attractive E3 ligase for expanding the scope of TPD approaches with tumor-specific activities.

Here, we report the discovery of a selective FBXO22 degrader and the subsequent optimization of an electrophilic warhead for FBXO22-mediated TPD. We serendipitously discovered that a primary amine contaminant generated during the synthesis of a PROTAC induced degradation of FBXO22. Structure-activity relationship studies of this compound identified the primary amine as being the essential degron. We constructed a small library of primary amine-derivatized CRBN- or VHL-based PROTACs, which was screened to identify the VHL-recruiting compound, AHPC(Me)-C6-NH_2 as the most potent FBXO22 degrader. Mechanistic studies demonstrated that metabolism of the primary amine to the corresponding aldehyde results in the formation of the biologically active AHPC-CHO. AHPC-CHO forms a reversible-covalent thioacetal with Cys326 of FBXO22 thereby stabilizing a ternary complex with VHL, which results in ubiquitination and subsequent proteosome-mediated degradation of FBXO22. We also discovered that simple diamino or dialdehyde alkanes can result in FBXO22 self-degradation. Lastly, during our efforts to improve self-degrader activity, we identified 2-pyridinecarboxaldehyde (2-PCA) as a novel reactive warhead for recruiting FBXO22 and developed degraders for targets including BRD4 and CDK12. Collectively, our findings provide a valuable chemical probe for investigating the biological function of FBXO22 and pave the way for more broadly harnessing FBXO22 for TPD.

RESULTS

E3 Ligand Tethered with Alkyl Amine Degrades FBXO22. As part of a chemical biology campaign to expand the degradable proteome, we used whole-cell proteomics to analyze the degradation profiles of our in-house PROTAC library. We observed that FBXO22 was the most prominently downregulated protein (P. Value <0.001, $\log_2$ fold change < -1.5) in both HEK293T and Kelly cells treated with ZXH-3-118 (Figures 1A, S1B, C). This compound is a byproduct generated during the synthesis of a WDR5 PROTAC molecule, which consists of a CRBN binder thalidomide,[39] a spacer, and a primary alkylamine (Figure S1A). We confirmed FBXO22 degradation in HEK293T, Kelly, and MOLT-4 cells (Figure S2A, B). Notably, this degradation was completely abolished upon depletion of fetal bovine serum (FBS) (Figure S2C), consistent with recent reports that amine oxidases present in FBS catalyze the metabolic conversion of primary alkylamine-containing compounds into their corresponding aldehyde analogs, thereby enabling engagement with FBXO22.[24,25] Based on these findings and the structural features of ZXH-3-118, we reasoned that an E3 ligase ligand combined with a primary amine group might be the minimal requirement for designing a degrader of FBXO22 (Figure 1A). Accordingly, we constructed a library of compounds containing various E3 ligase ligands (including CRBN, VHL, MDM2,[40] and IAP[41−44] and primary amine moieties with various linker lengths.

To facilitate compound screening, we established a HiBiT-FBXO22 assay by stably overexpressing FBXO22 fused to an N-terminal HiBiT-RR tag[45] in Jurkat cells. The engineered cell lines were treated with compounds across a range of concentrations for either 5 or 18 h, followed by end point measurement of target degradation using a luciferase assay. We initiated the screening with CRBN ligand-based compounds, as the original molecule containing a thalidomide ligand exhibited moderate activity. Simply attaching alkylamine of varying lengths to the 4-position of thalidomide via either O- or NH-linkages did not produce active FBXO22 degraders (Figure S3A, B). Considering that FBXO22 is also an E3 ligase, we used Western blot analysis to determine whether compounds could induce CRBN degradation but found no degradation of either protein (Figure S3C). Considering the structural similarity to ZXH-3-118, we hypothesized that incorporating a spacer might enhance molecular flexibility and improve activity. To test this, we prepared a series of thalidomide amido derivatives with different linker lengths. We found that linkers longer than C5 conferred moderate FBXO22 degradation activity, with a C8 linker compound achieving approximately 50% degradation at 3 μM after 5 h of treatment. In contrast, compounds with PEG linkers remained inactive (Figures 1B, S3D). Extending the treatment duration to 18 h did not further increase degradation efficacy. These results suggest that thalidomide tethered to primary alkylamine can induce moderate FBXO22 degradation, consistent with our observations for ZXH-3-118.

Next, we examined a series of VHL derivatives based on the AHPC ligand. While linkers shorter than C6 were inactive, the C6 derivative exhibited robust FBXO22 degradation, achieving approximately 70% degradation at 3 μM after 5 h (Figures 1C, S4). Longer treatment durations further increased the D_{max} to around 80%. Introducing a methyl group at the benzylic position, known to enhance VHL binding affinity, yielded an improved FBXO22 degrader that achieved approximately 80% degradation within 5 h. We also tested MDM2 and IAP ligand

https://doi.org/10.1021/jacs.5c14141
J. Am. Chem. Soc. XXXX, XXX, XXX−XXX

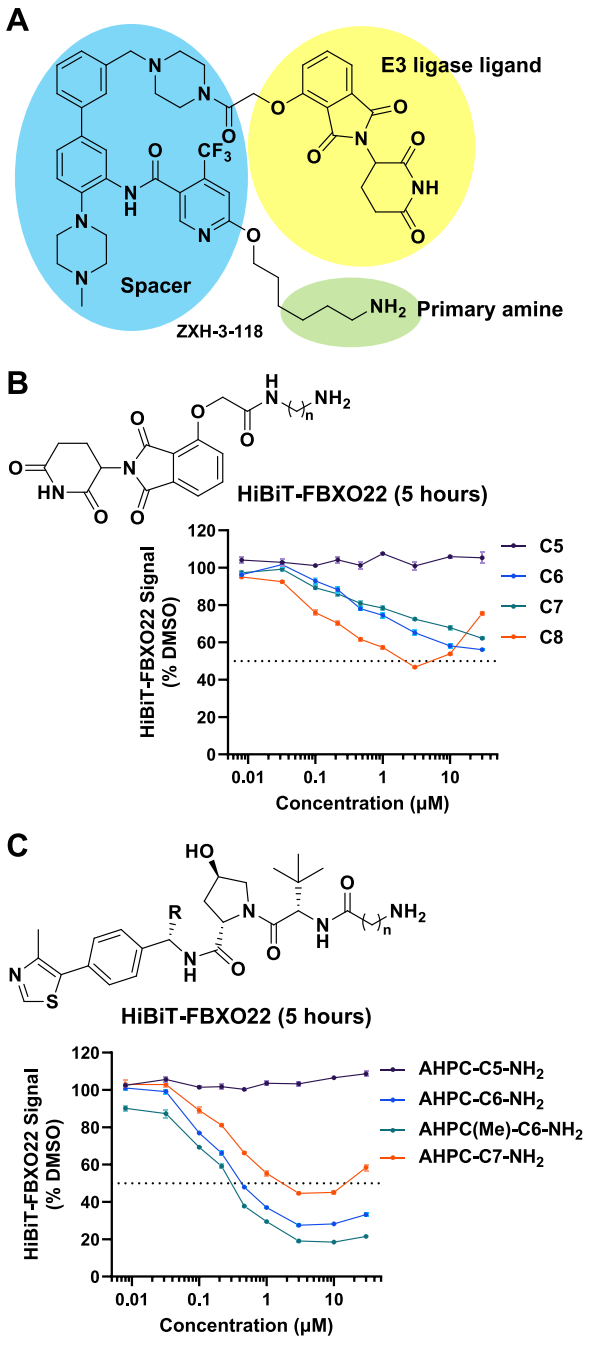

Figure 1. Charting E3 ligand tethered with primary amine for FBXO22 degradation. (A) Structure of ZXH-3-118. E3 ligase ligand is highlighted with yellow color, primary amine is highlighted with green color, and spacer region is highlighted with blue color. (B) General chemical structure of Thalidomide-Amide-Cn-NH_2 and HiBiT-FBXO22 assay results for Jurkat cells treated with the CRBN ligand-based degraders for 5 h. (C) General chemical structure of AHPC(R)-Cn-NH_2 and HiBiT-FBXO22 assay results for Jurkat cells treated with the VHL ligand-based degraders for 5 h.

tethered to hexylamine andneither induced FBXO22 degradation (Figure S5A, B). Based on these findings, we selected AHPC(Me)-C6-NH_2 (Figure 2A) as the lead FBXO22 degrader for further investigation.

AHPC(Me)-C6-NH_2 Is a Selective FBXO22 Degrader. To evaluate the degradation efficacy of AHPC(Me)-C6-NH_2 on endogenous FBXO22 protein, we conducted time- and dose-dependent experiments in Jurkat cells. The compound markedly induced the FBXO22 degradation at 1 μM over 5 h incubation, with a half-maximal degradation concentration (DC_{50}) of 77 nM and a D_{max} of 99% (Figure 2B, C). Treatment with 1 μM AHPC(Me)-C6-NH_2 resulted in FBXO22 degradation beginning as early as after 1 h, reaching the maximum degradation by 5 h, and persisted for at least 48 h (Figure 2D, E). Notably, VHL protein levels remained unaffected, indicating that in the context of FBXO22-VHL PROTACs, FBXO22 is the primary degradable target.

To assess selectivity, we carried out whole-cell proteomics on MOLT-4 cells treated with 1 μM of AHPC(Me)-C6-NH_2 for 5 h. Despite its structural simplicity, the degrader exhibited a highly selective degradation profile with FBXO22 being the only protein efficiently degraded across the entire proteome (Figure 2F). To evaluate the longer-term effects of FBXO22 degradation, we performed whole-cell proteomic analysis after 24 h of treatment with the FBXO22 degrader (Figure S6). At this time point, FBXO22 remained the most efficiently degraded protein. Notably, we also observed increased abundance of several lysine demethylases, including the known FBXO22 substrate KDM4A.[34,46] Collectively, these results confirm that AHPC(Me)-C6-NH_2 is a potent and highly selective chemical degrader of endogenous FBXO22.

Investigation of the Mechanism of AHPC(Me)-C6-NH_2 Induced FBXO22 Degradation. To investigate the mechanism underlying AHPC(Me)-C6-NH_2 induced FBXO22 degradation, we integrated chemical synthesis and pathway inhibition experiments to assess the roles of the UPS pathway and primary amine metabolic conversion. First, we synthesized two negative control compounds, ZZ7-23-033 and ZZ7-23-034, which feature either a secondary amine (resistant to oxidation to the aldehyde) or an inverted stereocenter (preventing VHL binding) (Figure 3A). Both compounds failed to induce FBXO22 degradation, indicating that both VHL engagement and a primary amine are required for activity (Figures 3B, S7A). Next, pretreatment with UPS pathway inhibitors, including TAK-243 (E1 inhibitor), MLN4924 (neddylation activating enzyme inhibitor), MG132 and bortezomib (proteasome inhibitors), blocked FBXO22 degradation. Additionally, preincubation with excess VHL ligand (VH032) abolished FBXO22 degradation, confirming the requirement for VHL recruitment. Lastly, we used two conditions to demonstrate the necessity of metabolic activation: (1) pretreatment with aminoguanidine (AG), a pan-amine oxidase inhibitor,[47] blocked FBXO22 degradation in the presence of FBS; and (2) switching from FBS-containing medium to Opti-MEM, which lacks FBS, also prevented degradation (Figures 3C, S7B).

Based on two previous studies demonstrating that primary amine-containing degraders are metabolized to the corresponding biologically active aldehydes, we first used LC-MS and HPLC to confirm AHPC(Me)-C6-NH_2 can be converted to the corresponding aldehyde in the presence of FBS, despite a low conversion rate (Figure S8A,B). Next, we synthesized a series of VHL ligand tethered alkyl aldehyde compounds with varying linker lengths (Figures 3A, S9A). In cellular assays, the analog equivalent to AHPC(Me)-C6-NH_2, namely AHPC-CHO, displayed the highest potency (DC_{50} = 150 nM, D_{max} = 72%). Analogs lacking a linker (ZZ7-24-008) or with a linker shortened by one carbon (TWQ-07-040) were inactive, indicating a minimal linker length requirement for effective FBXO22 degradation. An analogue with a linker extended by one carbon (TWQ-07-041) showed slightly improved efficacy at

https://doi.org/10.1021/jacs.5c14141
J. Am. Chem. Soc. XXXX, XXX, XXX−XXX

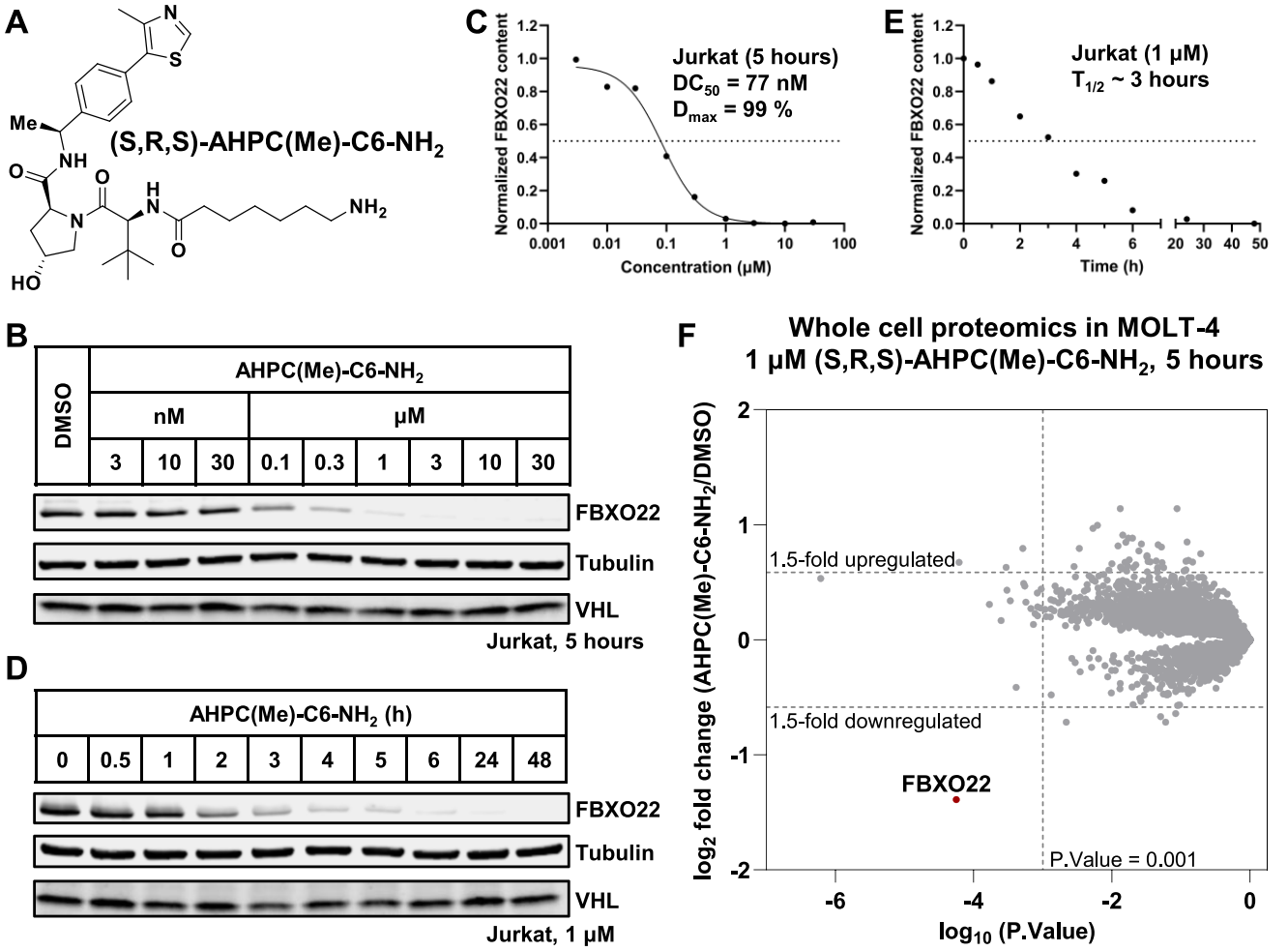

Figure 2. (S,R,S)-AHPC(Me)-C6-NH_2 is a potent and selective FBXO22 degrader. (A) Chemical structure of AHPC(Me)-C6-NH_2. (B) Western blots showing FBXO22 degradation in Jurkat cells treated with the indicated concentration of AHPC(Me)-C6-NH_2 for 5 h. (C) Quantification of the data shown in (B). (D) Western blots showing FBXO22 degradation in Jurkat cells treated with 1 μM AHPC(Me)-C6-NH_2 at indicated time. (E) Quantification of the data shown in (D). (F) Quantitative proteome-wide mass spectrometry in MOLT-4 cells after 5 h treatment with 1 μM AHPC(Me)-C6-NH_2.

low concentrations, but the D_{max} only reached 50% (Figure S9B, C). As expected, AHPC-CHO–mediated degradation was blocked by UPS pathway inhibitors, whereas switching to the FBS-free Opti-MEM medium had no impact (Figure S9D). In addition, AHPC-CHO outperformed its alkylamine analog at low concentrations but exhibited a more pronounced hook effect, a phenomenon often observed with PROTACs. These findings suggest that conversion of the amine into the aldehyde in FBS-containing medium serves as a prodrug mechanism, maintaining an optimal concentration of the active species to enable sustained FBXO22 degradation.

Building on this validation of AHPC-CHO as an active degrader, we next biochemically investigated its ability to form a ternary complex. To this end, we conducted a TR-FRET assay using four VHL-aldehyde compounds labeled VHL-EloB/C (VCB complex) and SKP1/FBXO22 (Figure S9E). Most compounds elicited a dose-dependent TR-FRET signal between 10 nM and 1 μM, with a hook effect observed at higher concentrations. In contrast, the linkerless compound ZZ7-24-008 produced negligible TR-FRET signal, only detectable at high concentrations. TWQ-07-040 showed the weakest TR-FRET signal, consistent with its lack of FBXO22 degradation and further supporting that an inadequate linker length impairs effective ternary complex formation. Previous reports suggested that alkyl aldehydes can engage cysteine 326 on FBXO22 to recruit FBXO22 for degradation of FKBP12 and NSD2.[24,25] We show that introducing a cysteine-to-alanine mutation at this site results in a near-complete loss of ternary complex formation between the VCB complex and SKP1/FBXO22 (Figure 3D). Together, these findings demonstrate that AHPC-CHO facilitates the formation of ternary complexes via cysteine 326 on FBXO22.

Given that whole-cell proteomics indicated high selectivity of AHPC(Me)-C6-NH_2 for degradation, we next investigated whether this selectivity originated from the preferred interaction between VHL and FBXO22 in the presence of a degrader. Using immunoprecipitation mass spectrometry (IP-MS),[48] we incubated MOLT-4 lysates with 1 μM AHPC-CHO and recombinant FLAG-tagged VCB complex. After one hour, the complex was enriched with Anti-FLAG M2 magnetic beads, followed by label-free quantitative proteomics to identify interactors (Figure 3E). Remarkably, only three proteins were significantly enriched (P. Value <0.001, $\log_2$ fold change > 2), with FBXO22 being the most enriched protein (P. Value = 4.7×10^{-9}, $\log_2$ fold change = 5.7) across the whole proteome. These findings support the idea that the observed degradation

https://doi.org/10.1021/jacs.5c14141
J. Am. Chem. Soc. XXXX, XXX, XXX−XXX

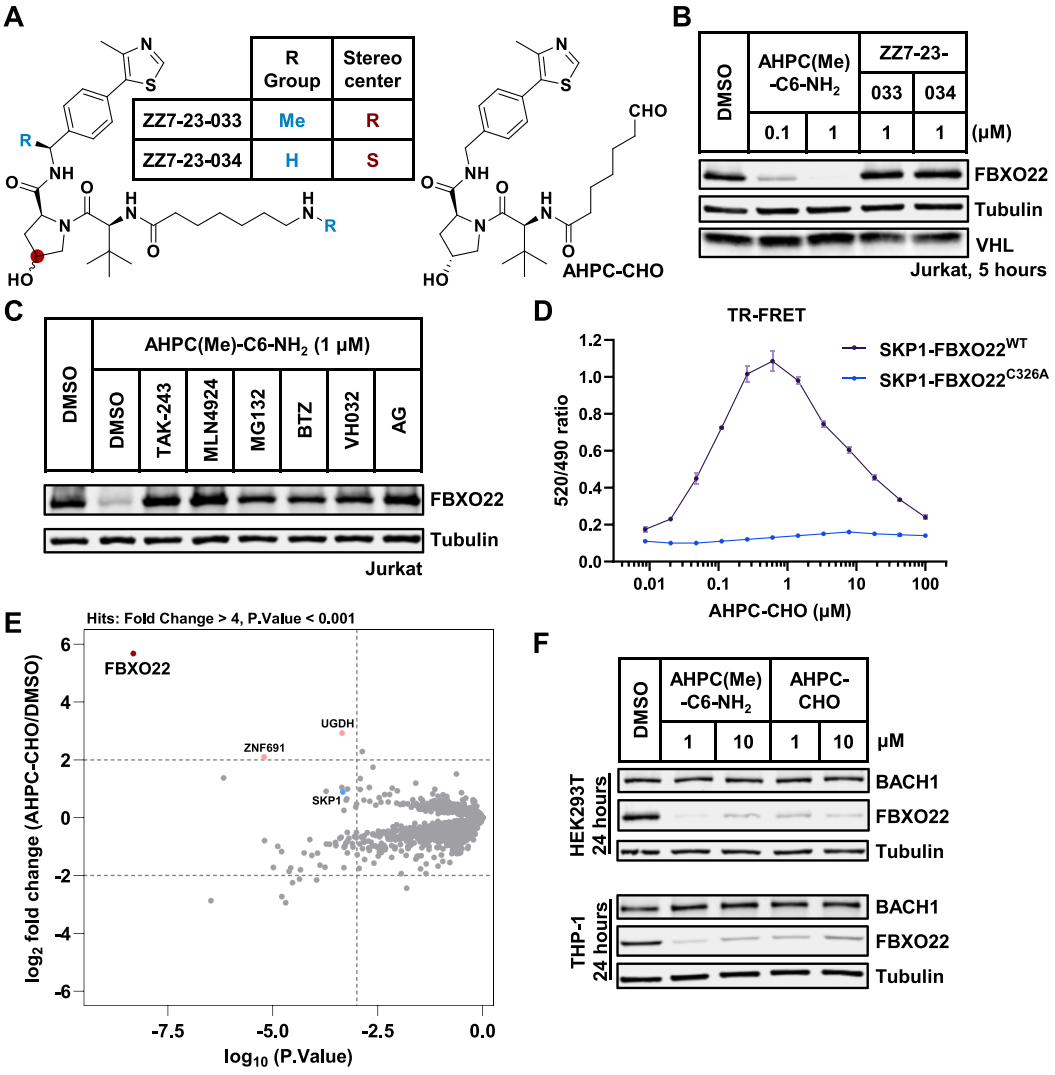

Figure 3. Mechanism of AHPC(Me)-C6-NH_2 induced FBXO22 degradation. (A) Chemical structures of ZZ7-23-033, ZZ7-23-034 and AHPC-CHO. (B) Western blots showing FBXO22 degradation in Jurkat cells treated with the indicated compounds for 5 h. (C) Western blots showing FBXO22 degradation in Jurkat cells pretreated with the indicated inhibitors for 1 h, followed by treatment with 1 μM AHPC(Me)-C6-NH_2 for 5 h. (D) TR-FRET assay to measure molecule-dependent ternary complex formation between VCB complex and SKP1/FBXO22 (WT or C326A). Each point represents a duplicate replicates; the mean value line is drawn. (E) Scatterplots depicting relative protein abundance following Flag-VHL-EloB/C enrichment from in-lysate treatment with 1 μM AHPC-CHO and recombinant Flag-VHL-EloB/C spike in. Scatterplots display fold change in abundance to DMSO. Significant changes were assessed by moderated *t* test as implemented in the limma package with $\log_2$ fold change shown on the *y*-axis and $\log_{10}$ (P. value) on the *x*-axis. (F) Western blots showing protein levels of FBXO22 and its downstream signals in HEK293T and THP-1 cells treated with indicated concentration of AHPC(Me)-C6-NH_2 and AHPC-CHO for 24 h.

selectivity arises from the specific recruitment of FBXO22 to the VCB complex.

Having confirmed the potency and selectivity of AHPC(Me)-C6-NH_2, we next assessed its activity in additional cell lines. Treatment of THP-1 and HEK293T cells with AHPC(Me)-C6-NH_2 and AHPC-CHO for 24 h resulted in robust FBXO22 degradation (Figures 3F, S9F). We also probed BACH1, a well-characterized substrate of FBXO22, to gain preliminary insight into the downstream effects. In THP-1 cells, we detected a modest increase in BACH1 protein levels, consistent with previous reports using genetic knockdown or knockout in this cell line.[32] Meanwhile, no clear changes in BACH1 were observed in HEK293T or Jurkat cells. Since there are no direct studies showing that FBXO22 loss affects endogenous BACH1 in these cell lines, we generated the FBXO22 knockout Jurkat cell line using CRISPR-Cas9 (Figure S10). Although FBXO22 was efficiently depleted, BACH1 protein levels remained unchanged, suggesting that other E3 ligases may regulate BACH1 stability in this context. Together, these results support the utility of AHPC(Me)-C6-NH_2 as a chemical biology tool to modulate FBXO22 levels and provide a foundation for future studies of FBXO22 function in diverse cellular environments.

Discovery of Primary Diamine as FBXO22 Self-Degrader. Symmetric homodimerizing PROTACs have been successfully developed for CRBN[49] and VHL.[23] We investigated whether a primary diamine could induce the self-degradation of FBXO22 (Figure 4A). To this end, we screened a series of primary diamines with varying linker lengths, along with their corresponding dialdehyde metabolites, using the HiBiT-FBXO22 assay (Figure 4B). Consistent with prior results for VHL- or CRBN-ligands tethered with alkylamines, primary diamines with C3−C5 linkers showed no activity (Figure 4C, S11A, and B). Although glutaraldehyde (1,5-pentanedial) demonstrated strong degradation activity in the HiBiT-

https://doi.org/10.1021/jacs.5c14141
J. Am. Chem. Soc. XXXX, XXX, XXX−XXX

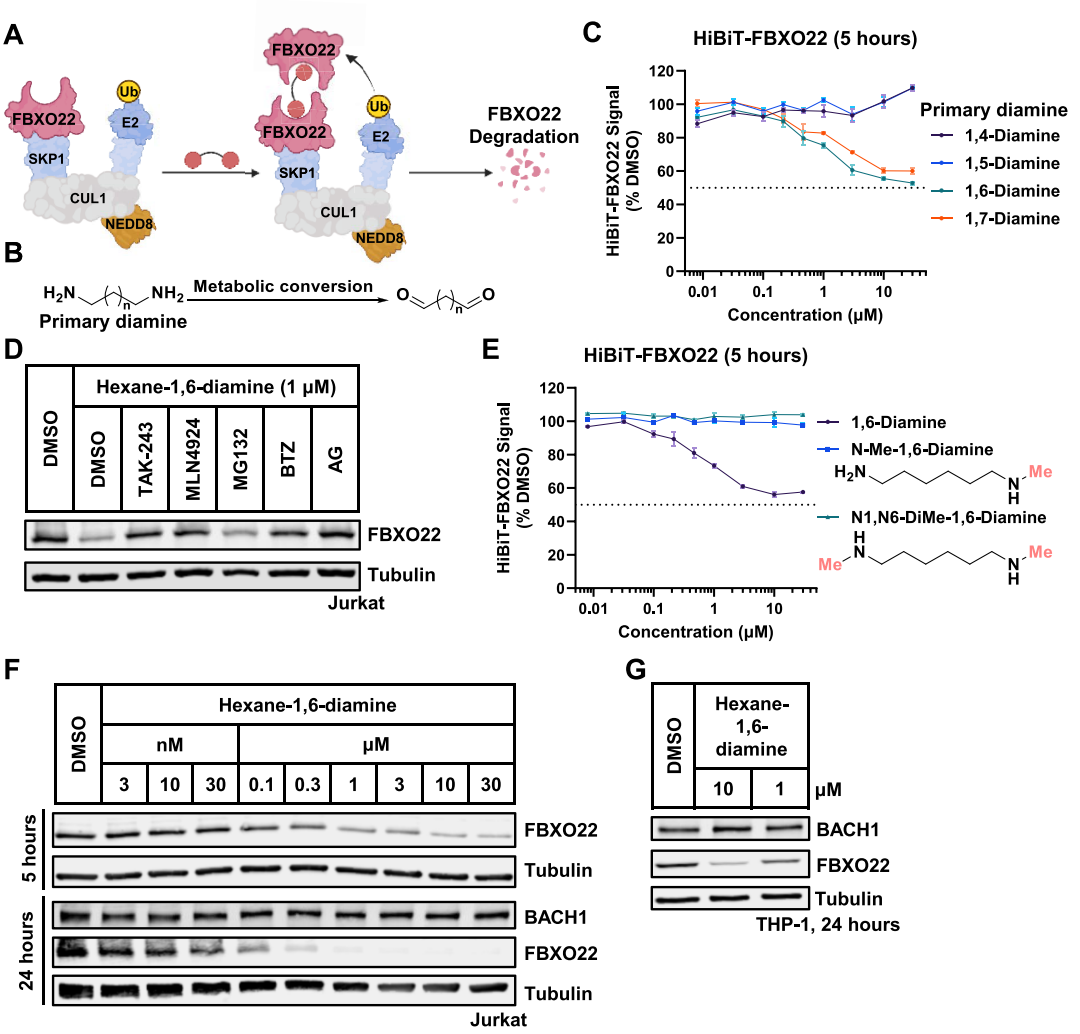

Figure 4. Primary diamine is FBXO22 self-degrader. (A) Schematic illustration showing the concept of FBXO22 self-degrader. (B) Metabolic conversion of primary diamine to dialdehyde. (C) HiBiT-FBXO22 assay results for Jurkat cells treated with the primary diamines for 5 h. (D) Western blots showing FBXO22 degradation in Jurkat cells pretreated with the indicated inhibitors for 1 h, followed by treatment with 1 μM hexane-1,6-diamine for 5 h. (E) HiBiT-FBXO22 assay results for Jurkat cells treated with methylated hexane-1,6-diamine for 5 h. (F) Western blots showing FBXO22 degradation in Jurkat cells treated with indicated concentration of hexane-1,6-diamine for 5 or 24 h. (G) Western blots showing protein levels of FBXO22 and its downstream signals in THP-1 cells treated with indicated concentration of hexane-1,6-diamine for 24 h.

FBXO22 assay (Figure S11C), it also caused cytotoxicity after 18 h, likely due to its known protein cross-linking properties (Figure S11D). Among the primary diamines tested, hexane-1,6-diamine exhibited the most potent degradation activity with a D_{max} of approximately 50% at 5 h, whereas its dialdehyde analog showed only marginal activity. Notably, compounds with linker lengths exceeding C7 lost activity dramatically, indicating that optimal linker length is critical for effective FBXO22 self-degradation.

To confirm that hexane-1,6-diamine–induced FBXO22 self-degradation is mediated by UPS, we pretreated the cells with UPS pathway inhibitors as described above and found that the FBXO22 degradation was largely blocked. Pretreatment with AG also reduced the FBXO22 degradation, indicating the metabolic conversion to aldehyde analog is required (Figure 4D). Furthermore, methylating one amine group to block its oxidation completely abolished FBXO22 degradation, suggesting that both primary amines must be converted to aldehydes to induce FBXO22 self-degradation (Figure 4E).

Given these results, we next examined whether hexane-1,6-diamine could induce the self-degradation of endogenous FBXO22. In Jurkat cells, treatment with hexane-1,6-diamine for 5 h led to dose-dependent FBXO22 degradation, achieving over 50% reduction at 1 μM. Extending incubation to 24 h substantially enhanced degradation, resulting in near-complete degradation at the same concentration (Figure 4F). Compared to AHPC(Me)-C6-NH_2, hexane-1,6-diamine exhibited a more pronounced dependency on incubation time, supporting the idea that metabolic conversion to aldehyde is a rate-determining step, as two deamination steps are required. Moreover, hexane-1,6-diamine did not alter BACH1 protein levels in Jurkat cells but increased BACH1 abundance in THP-1 cells, particularly at 10 μM, where FBXO22 degradation was more robust, indicating that the FBXO22 self-degrader is also biologically active (Figure 4G, S11E).

Charting Reactive Warheads for Hijacking FBXO22. While newly characterized E3 ligases offer opportunities for targeted protein degradation, their practical utility depends on the availability of effective ligands. Previous studies have

https://doi.org/10.1021/jacs.5c14141
J. Am. Chem. Soc. XXXX, XXX, XXX−XXX

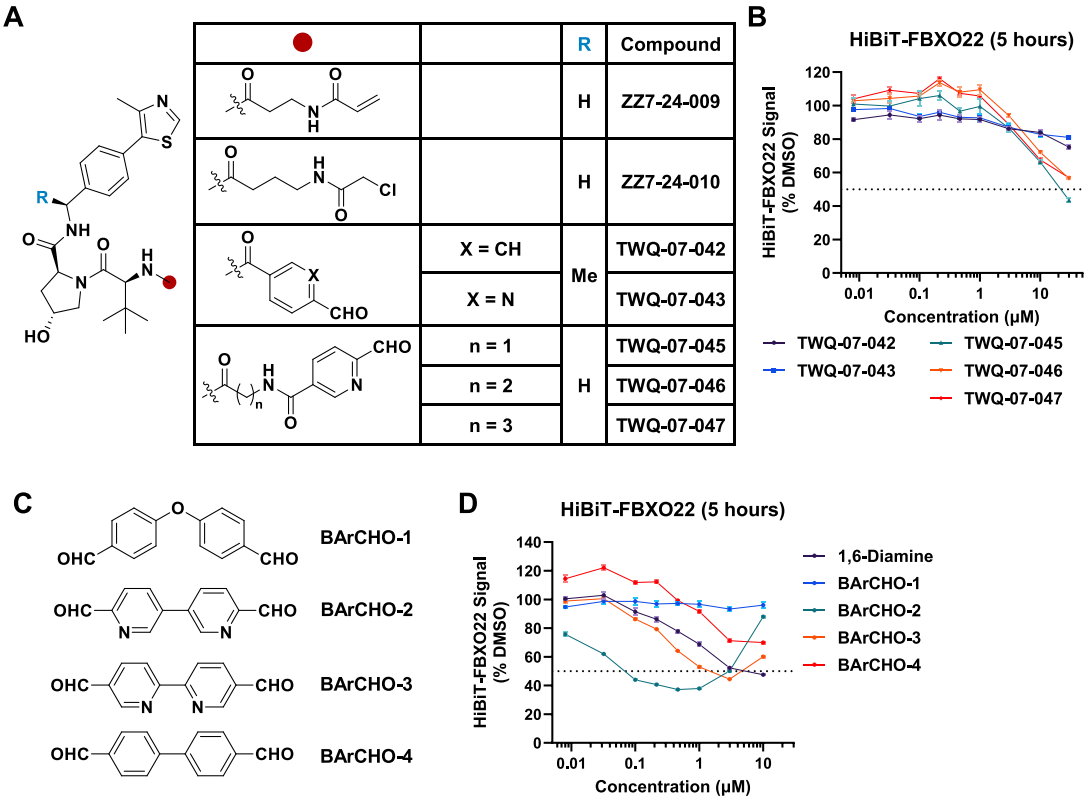

Figure 5. Charting cysteine reactive warhead for targeting FBXO22. (A) Chemical structure of VHL ligand tethered with various covalent warheads. (B) HiBiT-FBXO22 assay results for Jurkat cells treated with the VHL ligand-based degraders for 5 h. (C) Chemical structure of biaromatic dialdehyde (BArCHO). (D) HiBiT-FBXO22 assay results for Jurkat cells treated with the BArCHOs for 5 h.

documented the use of primary alkylamine or alkyl aldehyde as FBXO22 recruiters to degrade targets including NSD2,[24] XIAP,[50] FKBP12[25] and SMARCA2/A4.[28] FBXO22-mediated BRD4 degradation was successfully achieved using a chloroacetamide-based covalent fragment,[26] however, the primary amine tethering strategy proved ineffective, as confirmed by HiBiT assay results[25] (Figure S12). Hence, we next sought to explore novel warheads to more effectively harness FBXO22 in TPD applications.

Given that the reaction between thiols and aldehydes to form hemithioacetals is highly reversible, the resulting covalent engagement may lack sufficient stability to support processive ubiquitination. We hypothesized that enhancing the hemithioacetal stability could promote the formation of a FBXO22-containing ternary complex and thereby improve degradation efficacy, as shown in a recent study where a covalent cysteine warhead (chloroacetamide or acrylamide) engages C227/228 to recruit FBXO22 for a broader applicability in TPD.[26] Considering that AHPC(Me)-C6-NH_2 has proven effective for FBXO22 degradation by engaging Cys326, we installed various warheads on the VHL ligand and tested them in the HiBiT-FBXO22 assay. We first synthesized acrylamide (ZZ7-24-009) and chloroacetamide (ZZ7-24-010) analogs, two commonly used cysteine targeting covalent warheads. Despite having linker geometry similar to that of AHPC(Me)-C6-NH_2, neither compound induced degradation in the HiBiT-FBXO22 assay nor formed a ternary complex with the VCB complex and SKP1/FBXO22 (Figures 5A, S13A, B). Given that acrylamides and chloroacetamides are generally more reactive toward cysteine residues than alkyl aldehydes,[51] these results suggested that aldehyde functional group is essential for effective FBXO22 engagement.

To broaden the aldehyde repertoire, we focused on aromatic aldehydes, whose reactivity and stability can be better tuned through resonance and electronic effects.[52] We tested two representative aromatic aldehydes: benzaldehyde (BA) and 2-pyridinecarboxaldehyde (2-PCA). In our initial design, we installed aromatic aldehydes on the VHL recruiting ligand. We discovered that compounds with a spacer between the VHL ligand and 2-PCA exhibited modest dose-dependent FBXO22 degradation. Among them, TWQ-07-045, which features glycine as spacer, achieved approximately 50% D_{max} in the HiBiT-FBXO22 assay (Figures 5A, B, S14A). Encouraged by this, we hypothesized that biaromatic dialdehyde (BArCHO) could also facilitate FBXO22 self-degradation (Figure 5C). Indeed, the BArCHO-2 (3,3′-bipyridine-6,6′-dicarbaldehyde) displayed improved self-degradation with a DC_{50} below 0.1 μM and a D_{max} exceeding 60% in the HiBiT-FBXO22 assay. In contrast, bipyridine analogs containing 3-pyridine aldehyde (BArCHO-3) showed lower efficacy, and benzaldehyde derivatives were inactive (Figures 5D, S14B, C). The degradation efficacy correlated with the intrinsic reactivity of the aromatic aldehyde,[53] suggesting that aldehyde reactivity directly influences the FBXO22 self-degradation. Interestingly, despite the high reactivity of 2-PCA, neither BArCHO-2 nor TWQ-07-045 exhibited cytotoxicity (Figure S14D,E). Collectively, these findings identify 2-PCA as a promising alternative reactive warhead for targeting FBXO22.

2-Pyridinecarboxaldehyde Enables FBXO22-Mediated Targeted Protein Degradation. 2-PCA has been previously reported as a selective N-terminal protein labeling

https://doi.org/10.1021/jacs.5c14141
J. Am. Chem. Soc. XXXX, XXX, XXX−XXX

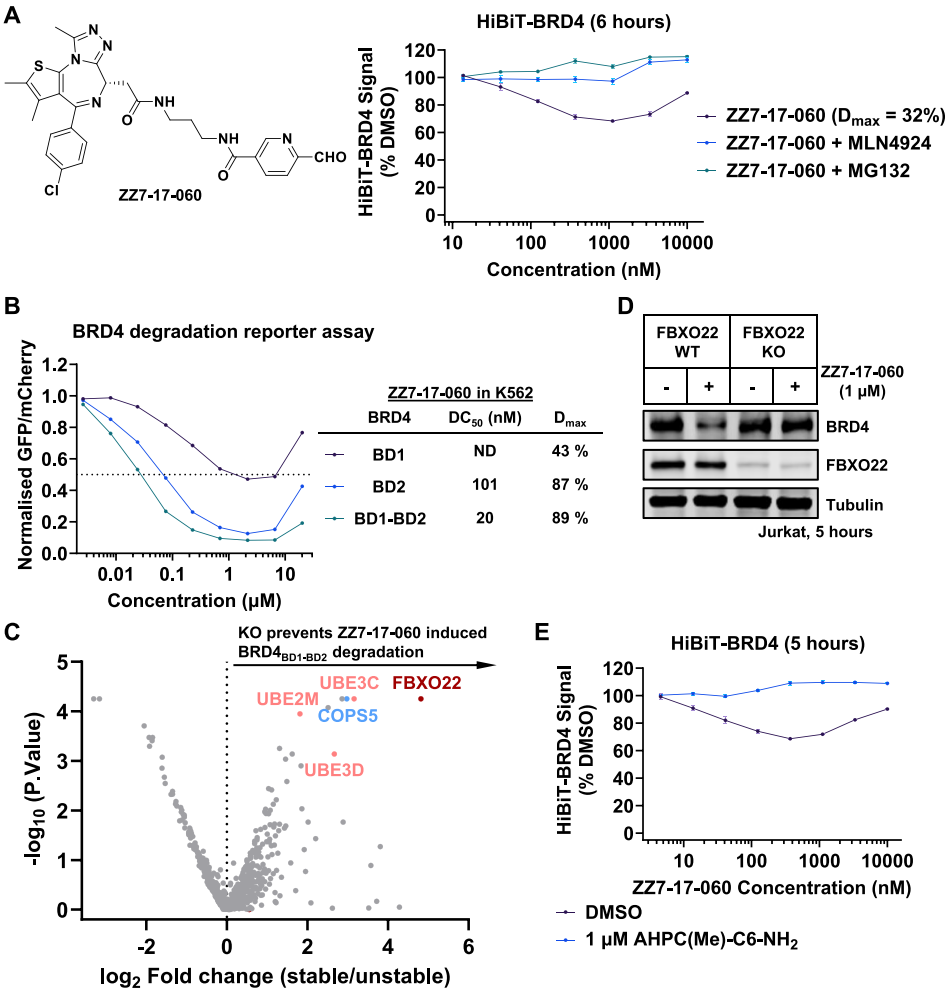

Figure 6. 2-Pyridinecarboxyaldehyde (2-PCA) enables FBXO22-mediated BRD4 degradation. (A) Chemical structure of ZZ7-17-060 and HiBiT-BRD4 assay results for Jurkat cells pretreated with the indicated inhibitors for 1.5 h, followed by treatment with ZZ7-17-060 for 6 h. (B) Identifying of the BRD4 region required for ZZ7-17-060−induced degradation with a cellular fluorescent reporter assay. The examined reporters were either the isolated BRD4 bromodomains (BD1 or BD2) or a tandem construct comprising BD1 and BD2 connected by the intervening native sequence ($BRD4_{BD1\text{-}BD2}$). (C) Ubiquitin-proteasome system (UPS)-focused CRISPR screen for $BRD4_{BD1\text{-}BD2}$-eGFP stability in K562-Cas9 cells treated with 10 μM ZZ7-17-060 for 16 h. Note the adaptor protein SKP1 is not in the BISON library. (D) Western blots showing BRD4 degradation in WT or FBXO22-KO Jurkat cells treated with 1 μM ZZ7-17-060 for 5 h. (E) HiBiT-BRD4 assay results for WT Jurkat cells pretreated with 1 μM AHPC(Me)-C6-NH_2, followed by treatment with ZZ7-17-060 for 5 h.

reagent used in protein conjugation chemistry,[54] but its utility in TPD has not been investigated. Building on the promising reactivity of 2-PCA as an FBXO22-directed warhead, we next investigated whether tethering 2-PCA to the BET bromodomain inhibitor JQ1[55] could enable BRD4 degradation, as JQ1 tethered with a primary alkylamine failed to induce BRD4 degradation.[25] We installed 2-PCA on JQ1 with linkers of varying lengths and measured BRD4 degradation activity using a HiBiT-BRD4 assay in Jurkat cells (Figure S15A). Remarkably, compounds with alkyl linkers exhibited degradation of BRD4, with ZZ7-17-060 (C3 linker) showing the highest potency, achieving a D_{max} value of around 32% (Figure 6A). Treatment with MLN4924 or MG132 blocked ZZ7-17-060−induced BRD4 degradation, suggesting that the effect is mediated by the UPS. We further synthesized several analogs with the optimal linker for SAR exploration. As expected, a benzaldehyde analog (ZZ7-24-036) showed no activity presumably due to its lower aldehyde reactivity. Similarly, swapping the amide with a sulfonamide (ZZ7-24-031) or pyridine with pyrimidine (ZZ7-24-030) also abolished the BRD4 degradation activity (Figure S15B). We reasoned that these modifications increased the reactivity of the aromatic aldehyde but also reduced its cellular stability, whereas 2-PCA achieves an optimal balance between reactivity and stability.

BRD4 contains two bromodomains (BDs),[56] and JQ1 binds both BDs with similar affinity.[55] To identify which region of BRD4 is responsible for ZZ7-17-060−induced degradation, we employed a fluorescent reporter assay to monitor BRD4 stability in K562 cells.[57] Reporters containing either bromodomain 2 (BRD4-BD2) alone or a tandem construct with both BD1 and BD2 showed strong degradation, with D_{max} exceeding 87%. In contrast, the BRD4-BD1 reporter displayed modest degradation with a D_{max} of approximately 43% (Figure 6B). Thus, ZZ7-17-060 harnesses both BDs, though preferably BRD4-BD2, for BRD4 degradation. Encouraged by the BRD4 degradation efficacy of ZZ7-17-060 in K562 cells, we performed whole-cell proteomics on K562 cells treated with 1 μM of ZZ7-17-060 for 3 h. Here we observed selective degradation of BET proteins (BRD2 and BRD4) across the proteome (Figure S16). Next, we used an unbiased screening approach to assess the 2-PCA

https://doi.org/10.1021/jacs.5c14141
J. Am. Chem. Soc. XXXX, XXX, XXX−XXX

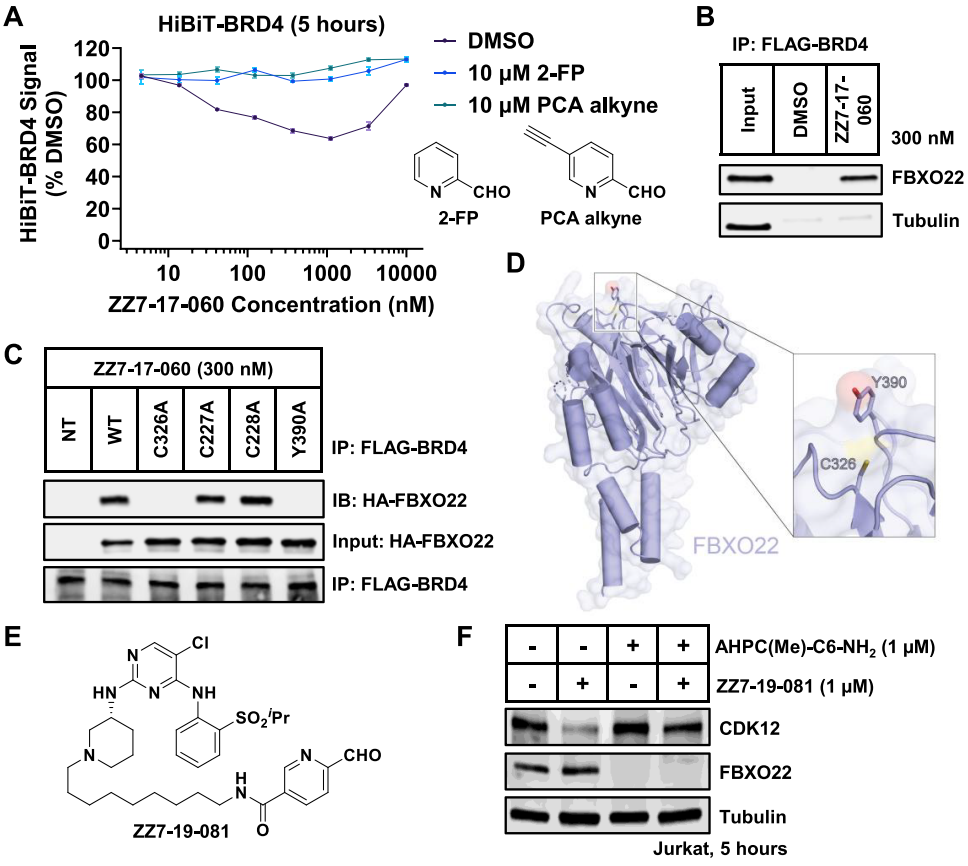

Figure 7. 2-PCA engages FBXO22 Cys326 to degrade target protein. (A) HiBiT-BRD4 assay results for Jurkat cells pretreated with 10 μM 2-FP or PCA-Alkyne for 1 h, followed by treatment with ZZ7-17-060 for 5 h. (B) Co-immunoprecipitation of FLAG-tagged BRD4 and endogenous FBXO22 in the presence of 300 nM ZZ7-17-060. (C) Co-immunoprecipitation of FLAG-tagged BRD4 and HA-FBXO22 (WT or mutations) in the presence of 300 nM ZZ7-17-060. NT indicates no transfection of FBXO22 constructs. (D) Schematic illustration of 2-PCA putative binding pocket on FBXO22 structure (PDB:8S7E). Cys326 and Tyr390 are highlighted in stick representation. (E) Chemical structure of CDK12 degrader ZZ7-19-081. (F) Western blots showing CDK12 degradation in Jurkat cells pretreated with 1 μM AHPC(Me)-C6-NH_2 for 1 h, followed by treatment with 1 μM ZZ7-19-081 for 5 h.

selectivity for E3 ligase recruitment. To this end, we conducted a fluorescence-activated cell sorting (FACS)-based CRISPR screen, targeting 713 genes involved in the UPS pathway.[58] Remarkably, FBXO22 emerged as the only significantly enriched E3 ligase, along with CUL1 and several candidate E2 enzymes (Figures 6C, S17). Consistent with this, genetic knockout or chemical knockdown of FBXO22 with AHPC(Me)-C6-NH_2 completely rescued the ZZ7-17-060–induced BRD4 degradation (Figures 6D, E, and S18). When reintroducing WT FBXO22 or the C326A mutant into FBXO22 knockout cells, the C326A mutant failed to restore ZZ7-17-060–mediated BRD4 degradation, suggesting that ZZ7-17-060 engages Cys326 on FBXO22 for BRD4 degradation (Figure S19).

To further elucidate the mechanism of ZZ7-17-060, and more broadly to assess whether 2-PCA directly binds to FBXO22, we investigated their interaction in more detail. First, we tested whether simple 2-PCA derivatives, 2-formylpyridine (2-FP) and PCA-alkyne, could compete with the activity of ZZ7-16-060 in inducing BRD4 degradation. Pretreatment with either compound completely abolished ZZ7-16-060–induced BRD4 degradation, suggesting that 2-PCA is capable of directly engaging FBXO22 (Figure 7A). Next, to confirm the formation of a new protein–protein interaction, we incubated ZZ7-17-060 with HEK293T lysates expressing FLAG-tagged BRD4 and observed the enrichment of FBXO22 only in the treatment group (Figure 7B). Further, we conducted similar IP experiments to test whether 2-PCA engages the same cysteine as the primary aldehyde and found that the C326A mutation completely prohibited FBXO22 engagement (Figure 7C). Interestingly, we noticed Y390 positioned close to C326, which may participate in ligand binding. Indeed, the Y390A mutation also completely abolished association of FBXO22 with BRD4 (Figure 7D). In addition, the Y390A mutation also prevented FBXO22 degradation by self-degraders (Figure S20A) and AHPC-CHO–mediated FBXO22-VHL interaction (Figure S20B), highlighting the importance of Y390 in facilitating the aldehyde-containing molecule mediated protein–protein interaction.

Finally, to probe the generality of FBXO22 recruitment to diverse targets, we tethered 2-PCA to a parental CDK12 inhibitor from the selective CDK12 degrader BSJ-4-116 via an alkyl linker (Figure 7E).[59] The resulting compound, ZZ7-19-081, exhibited modest CDK12 degradation, which was rescued by the chemical knockdown of FBXO22 with AHPC(Me)-C6-NH_2, indicating that FBXO22 mediates ZZ7-19-081–induced CDK12 degradation (Figure 7F). Together, these results further support 2-PCA as a selective degradation warhead that recruits FBXO22 for TPD.

https://doi.org/10.1021/jacs.5c14141
J. Am. Chem. Soc. XXXX, XXX, XXX–XXX

DISCUSSION

Recent reports investigating the mode of action of serendipitously discovered degraders have shown that FBXO22 can be hijacked for TPD using small molecules that function as prodrugs - compounds metabolically converted in cells to reactive aldehydes, enabling covalent engagement with FBXO22.[24−28] These studies established the proof of concept for FBXO22 as a ligandable E3 ligase but left open critical questions regarding direct engagement strategies, degradation selectivity, and the broader applicability of FBXO22 in induced proximity approaches.

In this work, we expand and deepen this emerging paradigm by developing the first direct chemical degraders of FBXO22 and systematically exploring their mechanisms of action. Our lead compound, AHPC(Me)-C6-NH_2, is a potent and selective degrader that mimics genetic loss of FBXO22 and serves as a chemical biology tool for probing its function. Comprehensive mechanistic studies, including SAR exploration, pathway inhibitor rescue experiments, and ternary complex formation assays—revealed its activity requires metabolic conversion of the primary amine into an alkyl aldehyde, consistent with prior reports that aldehyde-mediated covalent engagement enables FBXO22 recruitment. Despite its structural simplicity, AHPC-(Me)-C6-NH_2 exhibits remarkable proteome-wide selectivity for FBXO22 degradation. We hypothesized that this selectivity stems partially from the preferential protein−protein interaction between FBXO22 and VHL upon ternary complex formation, as FBXO22 emerges as the predominant protein in proximity to VHL upon treatment with the AHPC-CHO. While we also observed slight enrichment of SKP1 (log_2 fold change = 0.89) in the IP-MS analysis, the adaptor protein bridges FBXO22 and cullin-RING ligases (CRL), we did not detect other components of the CRL complex potentially due to the limiting cellular concentration of CUL1 to accommodate all F-box proteins.[60] This question could potentially be addressed using proximity labeling based approaches in future studies.[61,62] In addition, the aldehyde engages Cys326 of FBXO22 in a reversible covalent manner, whereas stronger covalent warheads failed to induce ternary complex formation or FBXO22 degradation, suggesting that FBXO22 selectivity also hinges on a finely balanced reversible engagement.

Building on this, we explored the concept of homo-PROTAC-mediated self-degradation, wherein E3 ligases are dimerized to induce their own ubiquitination and proteasomal degradation and identified hexane-1,6-diamine as a minimal self-degrader of FBXO22. In contrast, biologically relevant shorter-chain diamines such as putrescine (1,4-diaminobutane) and cadaverine (1,5-diaminopentane) lacked this activity.[63,64] The inability of these endogenous short-chain diamines to trigger FBXO22 degradation matches with their benign cellular roles and emphasizes the necessity of appropriate chain length and the related alkyl dialdehyde reactivity for effective FBXO22 recruitment and self-degradation. These insights mirror prior homo-PROTAC strategies used for VHL,[23] CRBN,[49] and MDM2[65] and highlight a potentially generalizable approach for chemically modulating E3 ligase levels. Given FBXO22's frequent overexpression in diverse cancers, the selective degraders we describe may offer starting points for therapeutic targeting of FBXO22-driven tumorigenic processes.

A key advance of our study is the discovery of 2-pyridinecarboxaldehyde (2-PCA) as a metabolically independent reactive warhead for FBXO22 recruitment. Unlike primary alkylamines, 2-PCA engages FBXO22 directly without requiring metabolic activation, enabling efficient FBXO22 self-degradation and degradation of diverse targets such as BRD4 and CDK12. This not only broadens the arsenal of electrophilic warheads available for TPD but also highlights the potential of aromatic aldehydes in designing selective, reversible E3 ligase recruiters. The effectiveness of 2-PCA−based degraders was reinforced by unbiased CRISPR screening, which confirmed FBXO22 as the sole E3 ligase required for the degradation of model protein BRD4. Given FBXO22's frequent overexpression in tumors, leveraging it as a recruiter may bias degrader activity toward cancer cells, offering a potential therapeutic advantage.

These findings collectively position FBXO22 as both a degradable protein target and a promising recruiter for induced proximity approaches. The toolkit we provide, comprising selective FBXO22 degraders, homo-PROTACs, and aromatic aldehyde-based warheads, complements and extends prior prodrug-based strategies by enabling direct, modular chemical control of FBXO22. Our results also highlight the broader principle that reversible covalent engagement, guided by intrinsic E3 ligase reactivity and proximity preferences, can unlock new opportunities for E3 ligase harnessing in TPD.

Despite 2-PCA and its derivatives having been reported to react specifically with N-terminal amino acid in peptides or proteins at high concentrations (~5 mM),[66,67] their utility in cysteine targeting remains rarely documented.[68] Our mutational analysis suggests that 2-PCA−based degraders recruit FBXO22 through Cys326 at substantially lower concentrations. Supporting this, both 2-FP and PCA-Alkyne fully rescued BRD4 degradation, suggesting that 2-PCA may directly bind to FBXO22. Attempts to capture the binding between FBXO22 and 2-PCA were not successful, likely due to the reversibility of the hemithioacetal linkage. Nevertheless, the robust neo-protein−protein interaction induced by ZZ7-17-060 and its potent activity against BRD4-BD2 support the feasibility of determining the structure of the BRD4-BD2/ZZ7-17-060/FBXO22 complex.

Looking forward, structural elucidation of FBXO22−ligand complexes and medicinal chemistry optimization of aromatic aldehyde warheads will be key to enhancing selectivity, potency, and substrate scope. Such advances could ultimately establish FBXO22 as a versatile alternative to canonical recruiter ligases such as CRBN and VHL, expanding the reach of TPD approaches in both mechanistic studies and therapeutic applications.

ASSOCIATED CONTENT

Data Availability Statement

Data generated in this study are provided in the manuscript, Supporting Information, and source data files. Additional data supporting the findings of this study are available from the corresponding author upon reasonable request.

Supporting Information

The Supporting Information is available free of charge at https://pubs.acs.org/doi/10.1021/jacs.5c14141.

Supporting figures, methods for biology, general information for chemistry, general procedure of preparing FBXO22 degraders, preparation of FBXO22 degraders, preparation of BRD4 degrader, preparation of CDK12 degrader and NMR spectra (PDF)

List of compound resources (XLSX)

Mass spectrometry and CRISPR screening data (XLSX)

https://doi.org/10.1021/jacs.5c14141
J. Am. Chem. Soc. XXXX, XXX, XXX−XXX

AUTHOR INFORMATION

Corresponding Authors

Nathanael S. Gray − *Department of Chemical and Systems Biology, ChEM-H and Stanford Cancer Institute, Stanford Medical School, Stanford University, Stanford, California 94305, United States;* orcid.org/0000-0001-5354-7403; Email: nsgray01@stanford.edu

Benjamin L. Ebert − *Department of Medical Oncology, Dana-Farber Cancer Institute, Boston, Massachusetts 02215, United States; Broad Institute of MIT and Harvard, Cambridge, Massachusetts 02142, United States;* Email: benjamin_ebert@dfci.harvard.edu

Authors

Tian Qiu − *Department of Chemical and Systems Biology, ChEM-H and Stanford Cancer Institute, Stanford Medical School, Stanford University, Stanford, California 94305, United States;* orcid.org/0000-0002-7168-0715

Zhe Zhuang − *Department of Chemical and Systems Biology, ChEM-H and Stanford Cancer Institute, Stanford Medical School, Stanford University, Stanford, California 94305, United States;* orcid.org/0000-0001-6679-0496

Woong Sub Byun − *Department of Chemical and Systems Biology, ChEM-H and Stanford Cancer Institute, Stanford Medical School, Stanford University, Stanford, California 94305, United States;* orcid.org/0000-0003-4676-3698

Zuzanna Kozicka − *Department of Medical Oncology, Dana-Farber Cancer Institute, Boston, Massachusetts 02215, United States; Broad Institute of MIT and Harvard, Cambridge, Massachusetts 02142, United States*

Kheewoong Baek − *Department of Cancer Biology, Dana-Farber Cancer Institute, Boston, Massachusetts 02215, United States; Department of Biological Chemistry and Molecular Pharmacology, Harvard Medical School, Boston, Massachusetts 02115, United States*

Jianing Zhong − *Department of Chemistry, Stanford University, Stanford, California 94305, United States*

Abby M. Thornhill − *Department of Cancer Biology, Dana-Farber Cancer Institute, Boston, Massachusetts 02215, United States*

Julia K. Ryan − *Department of Cancer Biology, Dana-Farber Cancer Institute, Boston, Massachusetts 02215, United States*

Katherine A. Donovan − *Department of Cancer Biology, Dana-Farber Cancer Institute, Boston, Massachusetts 02215, United States; Department of Biological Chemistry and Molecular Pharmacology, Harvard Medical School, Boston, Massachusetts 02115, United States;* orcid.org/0000-0002-8539-5106

Eric S. Fischer − *Department of Cancer Biology, Dana-Farber Cancer Institute, Boston, Massachusetts 02215, United States; Department of Biological Chemistry and Molecular Pharmacology, Harvard Medical School, Boston, Massachusetts 02115, United States;* orcid.org/0000-0001-7337-6306

Complete contact information is available at: https://pubs.acs.org/10.1021/jacs.5c14141

Author Contributions

[▽]T.Q., Z.Z., W.S.B., and Z.K. contributed equally.

Notes

The authors declare the following competing financial interest(s): Nathanael S. Gray is a founder, science advisory board member (SAB) and equity holder in Syros, C4, Allorion, Lighthorse, Voronoi, Inception, Matchpoint, Shenandoah (board member), Larkspur (board member) and Soltego (board member). The Gray lab receives or has received research funding from Novartis, Takeda, Astellas, Taiho, Jansen, Kinogen, Arbella, Deerfield, Springworks, Interline and Sanofi. Benjamin L. Ebert has received research funding from Novartis and Calico. He has received consulting fees from Abbvie. He is a member of the SAB and shareholder for Neomorph Inc., Big Sur Bio, Skyhawk Therapeutics, and Exo Therapeutics. Eric S. Fischer is a founder, SAB member, and equity holder of Civetta Therapeutics, Proximity Therapeutics, Neomorph, Inc. (also board of directors), Stelexis Biosciences, Inc., Anvia Therapeutics, Inc. (also board of directors), CPD4, Inc (also board of directors) and Nias Bio, Inc. He is an equity holder in Avilar Therapeutics, Ajax Therapeutics (also SAB), Photys Therapeutics (also SAB), and Lighthorse Therapeutics. E.S.F. is a consultant to Novartis, EcoR1 capital and Deerfield. The Fischer lab receives or has received research funding from Deerfield, Novartis, Ajax, Interline, Bayer and Astellas. Katherine A. Donovan receives or has received consulting fees from Neomorph Inc and Kronos Bio.

ACKNOWLEDGMENTS

This work was support by the National Institutes of Health (NIH) grants R01CA218278 (to N.S.G. and E.S.F.), R01CA262188 and R01CA214608 (both E.S.F.), NIH High End Instrumentation grant (1S10OD028697-01) (to N.S.G.), departmental funds from Stanford Chemical and Systems Biology and Stanford Cancer Institute (to N.S.G.), and Basic Science Research Program through the National Research Foundation of Korea (NRF) funded by the Ministry of Education (RS-2024-00410290) (to W.S.B.). B.L.E. received support for this work from the NIH (P01CA066996) and the Howard Hughes Medical Institute. Z.K. was supported by a Swiss National Science Foundation Postdoc. Mobility grant (P500PB_214385). K.B. is a Meghan E. Raveis Fellow of the Damon Runyon Cancer Research Foundation (DRG-2514-24). T.Q. thanks Dr. Stephen M. Hinshaw for helpful discussions.

REFERENCES

(1) Krone, M. W.; Crews, C. M. Next steps for targeted protein degradation. *Cell Chem. Biol.* **2025**, *32* (2), 219−226.

(2) Teng, M.; Gray, N. S. The rise of degrader drugs. *Cell Chem. Biol.* **2023**, *30* (8), 864−878.

(3) Cowan, A. D.; Ciulli, A. Driving E3 Ligase Substrate Specificity for Targeted Protein Degradation: Lessons from Nature and the Laboratory. *Annu. Rev. Biochem.* **2022**, *91*, 295−319.

(4) Békés, M.; Langley, D. R.; Crews, C. M. PROTAC targeted protein degraders: the past is prologue. *Nat. Rev. Drug Discov* **2022**, *21* (3), 181−200.

(5) Li, K.; Crews, C. M. PROTACs: past, present and future. *Chem. Soc. Rev.* **2022**, *51* (12), 5214−5236.

(6) Wang, B.; Cao, S.; Zheng, N. Emerging strategies for prospective discovery of molecular glue degraders. *Curr. Opin Struct Biol.* **2024**, *86*, 102811.

(7) Domostegui, A.; Nieto-Barrado, L.; Perez-Lopez, C.; Mayor-Ruiz, C. Chasing molecular glue degraders: screening approaches. *Chem. Soc. Rev.* **2022**, *51* (13), 5498−5517.

(8) Winter, G. E.; Buckley, D. L.; Paulk, J.; Roberts, J. M.; Souza, A.; Dhe-Paganon, S.; Bradner, J. E. Phthalimide conjugation as a strategy for in vivo target protein degradation. *Science* **2015**, *348* (6241), 1376−1381.

(9) Raina, K.; Lu, J.; Qian, Y.; Altieri, M.; Gordon, D.; Rossi, A. M.; Wang, J.; Chen, X.; Dong, H.; Siu, K.; et al. PROTAC-induced BET

protein degradation as a therapy for castration-resistant prostate cancer. *Proc. Natl. Acad. Sci. U. S. A.* **2016**, *113* (26), 7124−7129.
(10) Jevtić, P.; Haakonsen, D. L.; Rapé, M. An E3 ligase guide to the galaxy of small-molecule-induced protein degradation. *Cell Chem. Biol.* **2021**, *28* (7), 1000−1013.
(11) Belcher, B. P.; Ward, C. C.; Nomura, D. K. Ligandability of E3 Ligases for Targeted Protein Degradation Applications. *Biochemistry* **2023**, *62* (3), 588−600.
(12) Kannt, A.; Đikić, I. Expanding the arsenal of E3 ubiquitin ligases for proximity-induced protein degradation. *Cell Chem. Biol.* **2021**, *28* (7), 1014−1031.
(13) Kisselev, A. F.; van der Linden, W. A.; Overkleeft, H. S. Proteasome inhibitors: an expanding army attacking a unique target. *Chem. Biol.* **2012**, *19* (1), 99−115.
(14) Zheng, N.; Shabek, N. Ubiquitin Ligases: Structure, Function, and Regulation. *Annu. Rev. Biochem.* **2017**, *86*, 129−157.
(15) Padovani, C.; Jevtić, P.; Rapé, M. Quality control of protein complex composition. *Mol. Cell* **2022**, *82* (8), 1439−1450.
(16) Cruz Walma, D. A.; Chen, Z.; Bullock, A. N.; Yamada, K. M. Ubiquitin ligases: guardians of mammalian development. *Nat. Rev. Mol. Cell Biol.* **2022**, *23* (5), 350−367.
(17) Vassilev, L. T.; Vu, B. T.; Graves, B.; Carvajal, D.; Podlaski, F.; Filipovic, Z.; Kong, N.; Kammlott, U.; Lukacs, C.; Klein, C.; et al. In vivo activation of the p53 pathway by small-molecule antagonists of MDM2. *Science* **2004**, *303* (5659), 844−848.
(18) Oost, T. K.; Sun, C.; Armstrong, R. C.; Al-Assaad, A. S.; Betz, S. F.; Deckwerth, T. L.; Ding, H.; Elmore, S. W.; Meadows, R. P.; Olejniczak, E. T.; et al. Discovery of potent antagonists of the antiapoptotic protein XIAP for the treatment of cancer. *J. Med. Chem.* **2004**, *47* (18), 4417−4426.
(19) Chessari, G.; Buck, I. M.; Day, J. E.; Day, P. J.; Iqbal, A.; Johnson, C. N.; Lewis, E. J.; Martins, V.; Miller, D.; Reader, M.; et al. Fragment-Based Drug Discovery Targeting Inhibitor of Apoptosis Proteins: Discovery of a Non-Alanine Lead Series with Dual Activity Against cIAP1 and XIAP. *J. Med. Chem.* **2015**, *58* (16), 6574−6588.
(20) Buckley, D. L.; Van Molle, I.; Gareiss, P. C.; Tae, H. S.; Michel, J.; Noblin, D. J.; Jorgensen, W. L.; Ciulli, A.; Crews, C. M. Targeting the von Hippel-Lindau E3 ubiquitin ligase using small molecules to disrupt the VHL/HIF-1α interaction. *J. Am. Chem. Soc.* **2012**, *134* (10), 4465−4468.
(21) Galdeano, C.; Gadd, M. S.; Soares, P.; Scaffidi, S.; Van Molle, I.; Birced, I.; Hewitt, S.; Dias, D. M.; Ciulli, A. Structure-guided design and optimization of small molecules targeting the protein-protein interaction between the von Hippel-Lindau (VHL) E3 ubiquitin ligase and the hypoxia inducible factor (HIF) alpha subunit with in vitro nanomolar affinities. *J. Med. Chem.* **2014**, *57* (20), 8657−8663.
(22) Davies, T. G.; Wixted, W. E.; Coyle, J. E.; Griffiths-Jones, C.; Hearn, K.; McMenamin, R.; Norton, D.; Rich, S. J.; Richardson, C.; Saxty, G.; et al. Monoacidic Inhibitors of the Kelch-like ECH-Associated Protein 1: Nuclear Factor Erythroid 2-Related Factor 2 (KEAP1:NRF2) Protein-Protein Interaction with High Cell Potency Identified by Fragment-Based Discovery. *J. Med. Chem.* **2016**, *59* (8), 3991−4006.
(23) Maniaci, C.; Hughes, S. J.; Testa, A.; Chen, W.; Lamont, D. J.; Rocha, S.; Alessi, D. R.; Romeo, R.; Ciulli, A. Homo-PROTACs: bivalent small-molecule dimerizers of the VHL E3 ubiquitin ligase to induce self-degradation. *Nat. Commun.* **2017**, *8* (1), 830.
(24) Nie, D. Y.; Tabor, J. R.; Li, J.; Kutera, M.; St-Germain, J.; Hanley, R. P.; Wolf, E.; Paulakonis, E.; Kenney, T. M. G.; Duan, S.; et al. Recruitment of FBXO22 for targeted degradation of NSD2. *Nat. Chem. Biol.* **2024**, *20* (12), 1597−1607.
(25) Kagiou, C.; Cisneros, J. A.; Farnung, J.; Liwocha, J.; Offensperger, F.; Dong, K.; Yang, K.; Tin, G.; Horstmann, C. S.; Hinterndorfer, M.; et al. Alkylamine-tethered molecules recruit FBXO22 for targeted protein degradation. *Nat. Commun.* **2024**, *15* (1), 5409.
(26) Basu, A. A.; Zhang, C.; Riha, I. A.; Magassa, A.; Campos, M. A.; Caldwell, A. G.; Ko, F.; Zhang, X. A CRISPR activation screen identifies FBXO22 supporting targeted protein degradation. *Nat. Chem. Biol.* **2024**, *20* (12), 1608−1616.
(27) Zhang, X.; Simon, G. M.; Cravatt, B. F. Implications of frequent hitter E3 ligases in targeted protein degradation screens. *Nat. Chem. Biol.* **2025**, *21* (4), 474−481.
(28) Villemure, E.; Januario, T.; Zeng, M.; Budayeva, H. G.; Walters, B. T.; Lictao, A.; Li, K. S.; Ye, X.; Gilchrist, C. L.; Hoag, B.; et al. Rational design of potent small-molecule SMARCA2/A4 degraders acting via the recruitment of FBXO22. *Nat. Commun.* **2025**, *16* (1), 9679.
(29) Zhang, L.; Chen, J.; Ning, D.; Liu, Q.; Wang, C.; Zhang, Z.; Chu, L.; Yu, C.; Liang, H. F.; Zhang, B.; et al. FBXO22 promotes the development of hepatocellular carcinoma by regulating the ubiquitination and degradation of p21. *J. Exp Clin Cancer Res.* **2019**, *38* (1), 101.
(30) Ge, M. K.; Zhang, N.; Xia, L.; Zhang, C.; Dong, S. S.; Li, Z. M.; Ji, Y.; Zheng, M. H.; Sun, J.; Chen, G. Q.; et al. FBXO22 degrades nuclear PTEN to promote tumorigenesis. *Nat. Commun.* **2020**, *11* (1), 1720.
(31) Sun, R.; Xie, H. Y.; Qian, J. X.; Huang, Y. N.; Yang, F.; Zhang, F. L.; Shao, Z. M.; Li, D. Q. FBXO22 Possesses Both Protumorigenic and Antimetastatic Roles in Breast Cancer Progression. *Cancer Res.* **2018**, *78* (18), 5274−5286.
(32) Zhu, X. N.; Wei, Y. S.; Yang, Q.; Liu, H. R.; Zhi, Z.; Zhu, D.; Xia, L.; Hong, D. L.; Yu, Y.; Chen, G. Q. FBXO22 promotes leukemogenesis by targeting BACH1 in MLL-rearranged acute myeloid leukemia. *J. Hematol Oncol* **2023**, *16* (1), 9.
(33) Chen, S.; Ma, S.; Yan, J.; Wang, H.; Ding, B.; Guo, Z.; Ma, Y.; Chen, X.; Wang, Y. Pan-Cancer Analyses Reveal Oncogenic Role and Prognostic Value of F-Box Only Protein 22. *Front Oncol* **2022**, *11*, 790912.
(34) Tan, M. K.; Lim, H. J.; Harper, J. W. SCF(FBXO22) regulates histone H3 lysine 9 and 36 methylation levels by targeting histone demethylase KDM4A for ubiquitin-mediated proteasomal degradation. *Mol. Cell. Biol.* **2011**, *31* (18), 3687−3699.
(35) Johmura, Y.; Maeda, I.; Suzuki, N.; Wu, W.; Goda, A.; Morita, M.; Yamaguchi, K.; Yamamoto, M.; Nagasawa, S.; Kojima, Y.; et al. Fbxo22-mediated KDM4B degradation determines selective estrogen receptor modulator activity in breast cancer. *J. Clin Invest* **2018**, *128* (12), 5603−5619.
(36) Lignitto, L.; LeBoeuf, S. E.; Homer, H.; Jiang, S.; Askenazi, M.; Karakousi, T. R.; Pass, H. I.; Bhutkar, A. J.; Tsirigos, A.; Ueberheide, B.; et al. Nrf2 Activation Promotes Lung Cancer Metastasis by Inhibiting the Degradation of Bach1. *Cell* **2019**, *178* (2), 316−329.
(37) Cao, S.; Garcia, S. F.; Shi, H.; James, E. I.; Kito, Y.; Mao, H.; Kaisari, S.; Rona, G.; Deng, S.; Goldberg, H. V.; et al. Recognition of BACH1 quaternary structure degrons by two F-box proteins under oxidative stress. *Cell* **2024**, *187* (26), 7568−7584.
(38) Goretzki, B.; Khoshouei, M.; Schröder, M.; Penner, P.; Egger, L.; Stephan, C.; Argoti, D.; Dierlamm, N.; Rada, J. M.; Kapps, S.; et al. Dual BACH1 regulation by complementary SCF-type E3 ligases. *Cell* **2024**, *187* (26), 7585−7602.
(39) Sievers, Q. L.; Petzold, G.; Bunker, R. D.; Renneville, A.; Słabicki, M.; Liddicoat, B. J.; Abdulrahman, W.; Mikkelsen, T.; Ebert, B. L.; Thomä, N. H. Defining the human C2H2 zinc finger degrome targeted by thalidomide analogs through CRBN. *Science* **2018**, *362* (6414), eaat0572.
(40) Shibata, N.; Nagai, K.; Morita, Y.; Ujikawa, O.; Ohoka, N.; Hattori, T.; Koyama, R.; Sano, O.; Imaeda, Y.; Nara, H.; et al. Development of Protein Degradation Inducers of Androgen Receptor by Conjugation of Androgen Receptor Ligands and Inhibitor of Apoptosis Protein Ligands. *J. Med. Chem.* **2018**, *61* (2), 543−575.
(41) Sekine, K.; Takubo, K.; Kikuchi, R.; Nishimoto, M.; Kitagawa, M.; Abe, F.; Nishikawa, K.; Tsuruo, T.; Naito, M. Small molecules destabilize cIAP1 by activating auto-ubiquitylation. *J. Biol. Chem.* **2008**, *283* (14), 8961−8968.
(42) Chen, K. F.; Lin, J. P.; Shiau, C. W.; Tai, W. T.; Liu, C. Y.; Yu, H. C.; Chen, P. J.; Cheng, A. L. Inhibition of Bcl-2 improves effect of LCL161, a SMAC mimetic, in hepatocellular carcinoma cells. *Biochem. Pharmacol.* **2012**, *84* (3), 268−277.
(43) Shah, R. R.; Redmond, J. M.; Mihut, A.; Menon, M.; Evans, J. P.; Murphy, J. A.; Bartholomew, M. A.; Coe, D. M. Hi-JAK-ing the

https://doi.org/10.1021/jacs.5c14141
J. Am. Chem. Soc. XXXX, XXX, XXX−XXX

ubiquitin system: The design and physicochemical optimization of JAK PROTACs. *Bioorg. Med. Chem.* **2020**, *28* (5), 115326.
(44) Schiemer, J.; Horst, R.; Meng, Y.; Montgomery, J. I.; Xu, Y.; Feng, X.; Borzilleri, K.; Uccello, D. P.; Leverett, C.; Brown, S.; et al. Snapshots and ensembles of BTK and cIAP1 protein degrader ternary complexes. *Nat. Chem. Biol.* **2021**, *17* (2), 152−160.
(45) Lin, H.; Riching, K.; Lai, M. P.; Lu, D.; Cheng, R.; Qi, X.; Wang, J. Lysineless HiBiT and NanoLuc Tagging Systems as Alternative Tools for Monitoring Targeted Protein Degradation. *ACS Med. Chem. Lett.* **2024**, *15* (8), 1367−1375.
(46) Johmura, Y.; Sun, J.; Kitagawa, K.; Nakanishi, K.; Kuno, T.; Naiki-Ito, A.; Sawada, Y.; Miyamoto, T.; Okabe, A.; Aburatani, H.; et al. SCF(Fbxo22)-KDM4A targets methylated p53 for degradation and regulates senescence. *Nat. Commun.* **2016**, *7*, 10574.
(47) Gahl, W. A.; Pitot, H. C. Reversal by aminoguanidine of the inhibition of proliferation of human fibroblasts by spermidine and spermine. *Chem. Biol. Interact* **1978**, *22* (1), 91−98.
(48) Baek, K.; Metivier, R. J.; Roy Burman, S. S.; Bushman, J. W.; Yoon, H.; Lumpkin, R. J.; Ryan, J. K.; Abeja, D. M.; Lakshminarayan, M.; Yue, H.; et al. Unveiling the hidden interactome of CRBN molecular glues. *Nat. Commun.* **2025**, *16* (1), 6831.
(49) Steinebach, C.; Lindner, S.; Udeshi, N. D.; Mani, D. C.; Kehm, H.; Köpff, S.; Carr, S. A.; Gütschow, M.; Krönke, J. Homo-PROTACs for the Chemical Knockdown of Cereblon. *ACS Chem. Biol.* **2018**, *13* (9), 2771−2782.
(50) den Besten, W.; Verma, K.; Yamazoe, S.; Blaquiere, N.; Phung, W.; Izrael-Tomasevic, A.; Mulvihill, M. M.; Helgason, E.; Prakash, S.; Goncharov, T.; et al. Primary Amine Tethered Small Molecules Promote the Degradation of X-Linked Inhibitor of Apoptosis Protein. *J. Am. Chem. Soc.* **2021**, *143* (28), 10571−10575.
(51) Petri, L.; Egyed, A.; Bajusz, D.; Imre, T.; Hetényi, A.; Martinek, T.; Ábrányi-Balogh, P.; Keserű, G. M. An electrophilic warhead library for mapping the reactivity and accessibility of tractable cysteines in protein kinases. *Eur. J. Med. Chem.* **2020**, *207*, 112836.
(52) Patel, D.; Huma, Z. E.; Duncan, D. Reversible Covalent Inhibition—Desired Covalent Adduct Formation by Mass Action. *ACS Chem. Biol.* **2024**, *19* (4), 824−838.
(53) Hilal, S. H.; Bornander, L. L.; Carreira, L. A. Hydration Equilibrium Constants of Aldehydes, Ketones and Quinazolines. *QSAR & Combinatorial Science* **2005**, *24* (5), 631−638.
(54) Bridge, H. N.; Leiter, W.; Frazier, C. L.; Weeks, A. M. An N terminomics toolbox combining 2-pyridinecarboxaldehyde probes and click chemistry for profiling protease specificity. *Cell Chem. Biol.* **2024**, *31* (3), 534−549.
(55) Filippakopoulos, P.; Qi, J.; Picaud, S.; Shen, Y.; Smith, W. B.; Fedorov, O.; Morse, E. M.; Keates, T.; Hickman, T. T.; Felletar, I.; et al. Selective inhibition of BET bromodomains. *Nature* **2010**, *468* (7327), 1067−1073.
(56) Shi, J.; Vakoc, C. R. The mechanisms behind the therapeutic activity of BET bromodomain inhibition. *Mol. Cell* **2014**, *54* (5), 728−736.
(57) Li, Y. D.; Ma, M. W.; Hassan, M. M.; Hunkeler, M.; Teng, M.; Puvar, K.; Rutter, J. C.; Lumpkin, R. J.; Sandoval, B.; Jin, C. Y.; et al. Template-assisted covalent modification underlies activity of covalent molecular glues. *Nat. Chem. Biol.* **2024**, *20* (12), 1640−1649.
(58) Słabicki, M.; Kozicka, Z.; Petzold, G.; Li, Y. D.; Manojkumar, M.; Bunker, R. D.; Donovan, K. A.; Sievers, Q. L.; Koeppel, J.; Suchyta, D.; et al. The CDK inhibitor CR8 acts as a molecular glue degrader that depletes cyclin K. *Nature* **2020**, *585* (7824), 293−297.
(59) Jiang, B.; Gao, Y.; Che, J.; Lu, W.; Kaltheuner, I. H.; Dries, R.; Kalocsay, M.; Berberich, M. J.; Jiang, J.; You, I.; et al. Discovery and resistance mechanism of a selective CDK12 degrader. *Nat. Chem. Biol.* **2021**, *17* (6), 675−683.
(60) Reitsma, J. M.; Liu, X.; Reichermeier, K. M.; Moradian, A.; Sweredoski, M. J.; Hess, S.; Deshaies, R. J. Composition and Regulation of the Cellular Repertoire of SCF Ubiquitin Ligases. *Cell* **2017**, *171* (6), 1326−1339.
(61) Branon, T. C.; Bosch, J. A.; Sanchez, A. D.; Udeshi, N. D.; Svinkina, T.; Carr, S. A.; Feldman, J. L.; Perrimon, N.; Ting, A. Y. Efficient proximity labeling in living cells and organisms with TurboID. *Nat. Biotechnol.* **2018**, *36* (9), 880−887.
(62) Yamanaka, S.; Horiuchi, Y.; Matsuoka, S.; Kido, K.; Nishino, K.; Maeno, M.; Shibata, N.; Kosako, H.; Sawasaki, T. A proximity biotinylation-based approach to identify protein-E3 ligase interactions induced by PROTACs and molecular glues. *Nat. Commun.* **2022**, *13* (1), 183.
(63) Kovács, T.; Mikó, E.; Vida, A.; Sebő, É.; Toth, J.; Csonka, T.; Boratkó, A.; Ujlaki, G.; Lente, G.; Kovács, P.; et al. Cadaverine, a metabolite of the microbiome, reduces breast cancer aggressiveness through trace amino acid receptors. *Sci. Rep* **2019**, *9* (1), 1300.
(64) Wójcik, W.; Łukasiewicz, M.; Puppel, K. Biogenic amines: formation, action and toxicity - a review. *J. Sci. Food Agric* **2021**, *101* (7), 2634−2640.
(65) He, S.; Ma, J.; Fang, Y.; Liu, Y.; Wu, S.; Dong, G.; Wang, W.; Sheng, C. Homo-PROTAC mediated suicide of MDM2 to treat non-small cell lung cancer. *Acta Pharm. Sin B* **2021**, *11* (6), 1617−1628.
(66) MacDonald, J. I.; Munch, H. K.; Moore, T.; Francis, M. B. One-step site-specific modification of native proteins with 2-pyridinecarboxyaldehydes. *Nat. Chem. Biol.* **2015**, *11* (5), 326−331.
(67) Griswold, A. R.; Cifani, P.; Rao, S. D.; Axelrod, A. J.; Miele, M. M.; Hendrickson, R. C.; Kentsis, A.; Bachovchin, D. A. A Chemical Strategy for Protease Substrate Profiling. *Cell Chem. Biol.* **2019**, *26* (6), 901−907.
(68) Fairhurst, R. A.; Knoepfel, T.; Buschmann, N.; Leblanc, C.; Mah, R.; Todorov, M.; Nimsgern, P.; Ripoche, S.; Niklaus, M.; Warin, N.; et al. Discovery of Roblitinib (FGF401) as a Reversible-Covalent Inhibitor of the Kinase Activity of Fibroblast Growth Factor Receptor 4. *J. Med. Chem.* **2020**, *63* (21), 12542−12573.

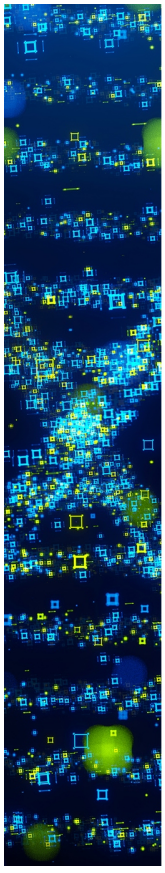

https://doi.org/10.1021/jacs.5c14141
J. Am. Chem. Soc. XXXX, XXX, XXX−XXX